ACADEMIC PRESS

Available online at www.sciencedirect.com

SCIENCE DIRECT®

Journal of Sound and Vibration 260 (2003) 783–805

JOURNAL OF SOUND AND VIBRATION

www.elsevier.com/locate/jsvi

Bifurcations and chaotic motions in the autonomous system of a restrained pipe conveying fluid

J.D. Jin*, G.S. Zou

Department of Engineering Mechanics, Shenyang Institute of Aeronautical Engineering, Shenyang 110034, People's Republic of China

Received 12 September 2001; accepted 8 May 2002

Abstract

The stability and dynamics of a cantilevered pipe conveying fluid with motion-limiting constraints and a linear spring support have been investigated. Emphasis is placed on analyzing local qualitative behavior of the system in the neighborhood of a doubly degenerate point. Using some qualitative reduction methods of dynamical system theory, the four-dimensional differential equation of motion is reduced to a two-dimensional one, and then the possible motions of the pipe are predicted through analyzing bifurcations of the solution to the reduced equation of motion. The unfolding result is found to be in good agreement with the result obtained using the numerical method. It is also found that there exist the quasi-periodic motions and route to chaos through breakup of the quasi-periodic torus surface in some parameter region of the system, which differs from that of periodic-doubling bifurcation route found earlier in this system. Numerical simulations have been performed using the four-dimensional equation of motion to confirm the analytical results.

1. Introduction

With the development of the theory on non-linear dynamical systems and chaos in recent years, much attention has been paid to the study of non-linear dynamics of pipes conveying fluid [1]. Some important phenomena, which have never been observed in the linear analysis of the systems, have been discovered [2]. Païdoussis and Moon studied, both experimentally and theoretically, the dynamics of a cantilevered pipe which is constrained by non-linear motion restraints. In a range of values of flow velocity beyond the Hopf bifurcation, they found that chaotic motions arise in this

*Corresponding author.
E-mail address: jinjd@163.com (J.D. Jin).

0022-460X/03/$ - see front matter
PII: S0022-460X(02)00982-3

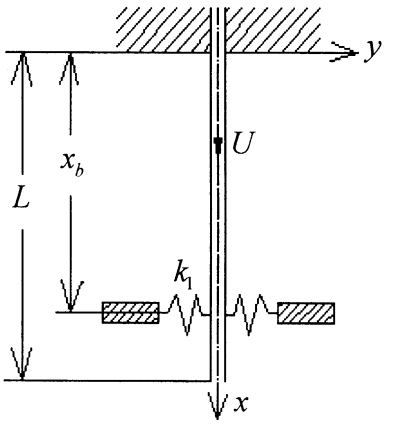

Fig. 1. Schematic of the system treated in this paper.

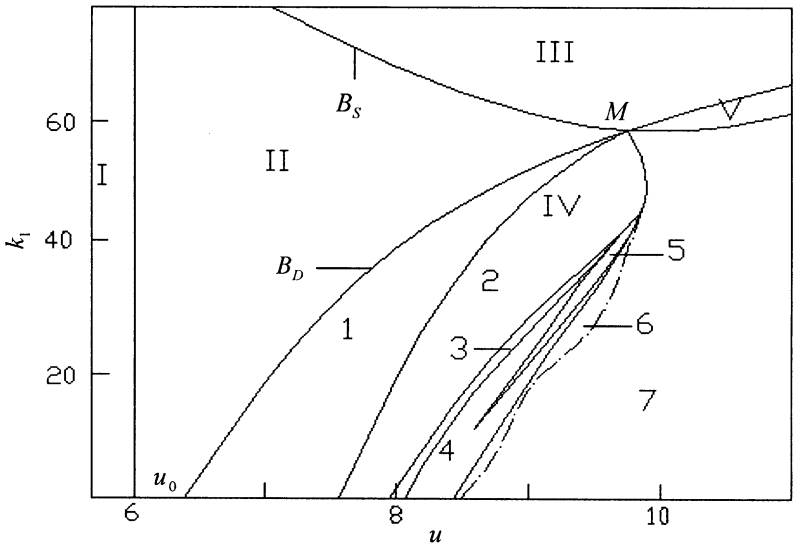

Fig. 2. Sketch of stability regions (redrawn from Ref. [6]).

autonomous system through the period-doubling bifurcations [2,3]. A series of further studies on this topic was done by Païdoussis et al. [4,5] from various aspects focusing on their attention to the characteristics of the chaotic motions. Recently, the authors studied the dynamics of a slightly modified system with the motion-limiting constraints and a linear spring support, as shown in Fig. 1 [6]. The effect of the linear spring constant (k_1) and flow velocity (u) on the motions of the pipe was mainly investigated by using the method of numerical simulations. It is found that the region of dynamic instability in (u–k_1) parameter plane may be divided into several sub-regions in each of which a different dynamical behavior including chaotic motions of the pipe arises (see Fig. 2).

As we see from Fig. 2, there is an intersection point M on the boundary of static and dynamic instability regions, and the boundary curves of the sub-regions in (u–k_1) plane all originate from

this intersection point. This allows us to think of a possible bifurcation of the solution at the point and expect some complicated behavior to occur in the neighborhood of that point. In fact, the zero equilibrium of the pipe is doubly degenerate at the point. The linearized matrix of equation of motion of the system at point M has a zero and a pair of pure imaginary eigenvalues, which corresponds to the coupled flutter and divergence bifurcation of the motion. This paper is concerned primarily with the stability and dynamics of the same restrained cantilevered pipe conveying fluid as treated in Ref. [6]. However, emphasis is placed on analyzing a codimension-two bifurcation problem and unfolding the double degeneracy at point M. The main purpose of this paper is to explain the results obtained in Ref. [6] from a viewpoint of bifurcation of solution. It should be pointed out that very laborious simulation analysis and much effort are needed indeed for determining the sub-regions in the "flutter region" and drawing Fig. 2. In order to do so, the parameter plane was divided into a network with certain steps of u and k_1, and numerical simulations were carried out by solving the equation of motion directly *at every net point*, and then, the behavior of the system at each net point was determined through observation of phase trajectories of the solutions. However, we will show, in this paper, that the same or even more refined results may also be obtained through analyzing the bifurcation of the solutions in the neighborhood of the doubly degenerate point.

2. Differential equation of motion and doubly degenerate system

The system considered here is shown in Fig. 1. The reader should refer to Ref. [6] for details for the mechanical model of the pipe and some assumptions needed for derivation of equation of motion. The differential equation of motion of the system can be written as [6]

$$aEI\frac{\partial^5 y}{\partial x^4\partial t}+EI\frac{\partial^4 y}{\partial x^4}+[MU^2-(M+m)(L-x)g_0]\frac{\partial^2 y}{\partial x^2}+2MU\frac{\partial^2 y}{\partial x\partial t}$$
$$+(M+m)g_0\frac{\partial y}{\partial x}+(M+m)\frac{\partial^2 y}{\partial t^2}+(K_1y+K_2y^3)\,\delta(x-x_b)=0, \tag{1}$$

where EI is the flexural rigidity of the pipe, a the coefficient of Kelvin–Voigt viscoelastic damping of the pipe material, L the pipe length and m its mass per unit length, M is the mass of the conveying fluid per unit length and U its flow velocity, K_1 is the stiffness of the spring of the elastic support and K_2 is the stiffness of cubic spring which represents the effect of the motion constraints, x_b the location of the constraints, g_0 is the acceleration due to gravity, $\delta(\cdot)$ is Dirac delta function, $y(x,t)$ is the lateral deflection of the pipe and assumed to be small compared with L.

Introducing the following non-dimensional variables and parameters:

$$W=\frac{y}{L},\qquad \xi=\frac{x}{L},\qquad \tau=\left(\frac{EI}{M+m}\right)^{1/2}\frac{t}{L^2},\qquad u=\left(\frac{M}{EI}\right)^{1/2}UL,\qquad \gamma=\frac{M+m}{EI}g_0L^3,$$
$$\beta=\frac{M}{M+m},\qquad \alpha=\left(\frac{EI}{M+m}\right)^{1/2}\frac{a}{L^2},\qquad k_1=K_1\frac{L^3}{EI},\qquad k_2=K_2\frac{L^5}{EI},\qquad \xi_b=\frac{x_b}{L}. \tag{2}$$

Eq. (1) may be rendered to a dimensionless form, and then can be discretized by Galerkin's technique. Let

$$W(\xi,\tau)=\sum_{i=1}^{2}\varphi_i(\xi)q_i(\tau),$$
$$\varphi_i(\xi)=\cosh(\lambda_i\xi)-\cos(\lambda_i\xi)-\sigma_i[\sinh(\lambda_i\xi)-\sin(\lambda_i\xi)], \tag{3}$$
$$\sigma_i=(\sinh\lambda_i-\sin\lambda_i)/(\cosh\lambda_i+\cos\lambda_i)\quad(i=1,\,2),$$
$$\lambda_1=1.875,\qquad \lambda_2=4.694,$$

where φ_i and $\lambda_i\,(i=1,2)$ are the eigenfunctions and eigenvalues of the cantilevered beam, respectively. Then, applying Galerkin's method, one obtains a four-dimensional ordinary differential equation of motion [6]:

$$\dot{X}=AX+F(X), \tag{4}$$

where

$$X=(x_1,x_2,x_3,x_4)^{\mathrm{T}},\qquad F(X)=(0,0,F_3,F_4)^{\mathrm{T}},$$
$$x_1=q_1,\qquad x_2=q_2,\qquad x_3=\dot{q}_1,\qquad x_4=\dot{q}_2,$$
$$A=\begin{bmatrix}0&0&1&0\\0&0&0&1\\a_1&a_2&a_3&a_4\\b_1&b_2&b_3&b_4\end{bmatrix}. \tag{5}$$

The detailed expressions for a_i, b_i $(i=1,2,3,4)$, F_3 and F_4 in Eqs. (5), and those of e, b_{sr}, c_{sr}, d_{sr}, e_{sr}, g_{sr} $(s,\,r=1,\,2)$ contained in these expressions can be found in Ref. [6] and are not repeated here.

In what follows, let $\gamma=10$, $\xi_b=0.82$, $k_2=100$ [3,6], while u,k_1,α,β are allowed to vary, and let $\mu=(u,k_1,\alpha,\beta)^{\mathrm{T}}$. Note that the matrix A in Eq. (4) is dependent on the parameter μ, but $F(x)$ is not. Rewriting A as A_μ for special emphasis to the dependence on μ, then Eq. (4) becomes

$$\dot{X}=A_\mu X+F(X). \tag{6}$$

The eigenvalue problem of A_μ yields a quartic characteristic equation of the form

$$\Omega^4+H_1\Omega^3+H_2\Omega^2+H_3\Omega+H_4=0, \tag{7}$$

where

$$H_1=-(a_3+b_4),$$
$$H_2=a_3b_4-b_3a_4-b_2-a_1,$$
$$H_3=a_1b_4-b_1a_4+b_2a_3-a_2b_3,$$
$$H_4=a_1b_2-b_1a_2.$$

Obviously, the coefficients $H_i\,(i=1,2,3,4)$ are dependent on the parameter μ. We analyze in this study the local behavior of the system for the parameter μ lying in the neighborhood of $\mu=\mu_0$

(corresponds to the intersection point M in Fig. 2) for which A_{μ_0} has a zero eigenvalue and a pair of pure imaginary eigenvalues, and the remaining eigenvalue of A_{μ_0} is assumed to be negative. The above assumptions require that three conditions must be satisfied: that is,

$$H_3 = H_1 H_2, \quad H_3 > 0, \tag{8}$$

$$H_4 = 0. \tag{9}$$

Solving Eq. (8) for k_1 and substituting it into Eq. (9), we may solve Eq. (9) for u, obtaining $u_0(\alpha, \beta)$. Substituting $u_0(\alpha, \beta)$ into Eq. (8) again, we may solve for k_1, obtaining $k_{10}(\alpha, \beta)$, and thus obtain

$$\mu_0 = (u_0(\alpha, \beta),\ k_{10}(\alpha, \beta),\ \alpha,\ \beta)^{\mathrm{T}}, \tag{10}$$

which is dependent on the parameters of α and β. Now we have the following degenerative eigenvalues of A_{μ_0}:

$$\Omega_{1,2} = \mp \mathrm{i}\omega_0, \qquad \Omega_3 = 0, \qquad \Omega_4 = -H_1 < 0. \tag{11}$$

Here $\omega_0 = \sqrt{H_3/H_1}$.

In order to investigate the local behavior of the system near μ_0, we introduce the local parameters

$$\delta = (\delta_1, \delta_2)^{\mathrm{T}},$$

where

$$\delta_1 = u - u_0, \qquad \delta_2 = k_1 - k_{10}. \tag{12}$$

Thus,

$$\mu = \mu_0 + (\delta_1, \delta_2, 0, 0)^{\mathrm{T}} \tag{13}$$

and Eq. (6) becomes

$$\dot{X} = A_\mu X + F(X) \equiv D_\delta X + F(X). \tag{14}$$

Note that Eq. (14) becomes a degenerate system in the case of $\delta = 0$.

3. Reduction of the system

The matrix A_{μ_0} can be put into Jordan normal form by a transformation matrix V that is composed of the eigenvectors of A_{μ_0}. Now we introduce the transformation

$$X = VY. \tag{15}$$

Substituting Eq. (15) into Eq. (14), one can obtain

$$\mathrm{d}Y/\mathrm{d}\tau = (J + \bar{A}_\delta)Y + f(Y), \tag{16}$$

where

$$J = \begin{bmatrix} J_c & 0 \\ 0 & J_d \end{bmatrix}, \qquad J_c = \begin{bmatrix} 0 & -\omega_0 & 0 \\ \omega_0 & 0 & 0 \\ 0 & 0 & 0 \end{bmatrix},$$
$$J_d = -\alpha(\lambda_1^4 + \lambda_2^4) - 2\sqrt{\beta}u(b_{11} + b_{22}),$$
$$\bar{A}_\delta = V^{-1}(D_\delta - D_0)V \equiv \begin{bmatrix} \bar{A}_{c1} & \bar{A}_{c2} \\ \bar{A}_{d1} & \bar{A}_{d2} \end{bmatrix},$$
$$f(Y) = V^{-1}F(VY) \equiv (f_c, f_d)^{\mathrm{T}}, \qquad Y = (y_c, y_d)^{\mathrm{T}}$$
$$y_c = (y_1, y_2, y_3)^{\mathrm{T}} \in \mathbb{R}^3 \qquad y_d = y_4 \in \mathbb{R}. \tag{17}$$

Note that the system considered here has a symmetry:

$$f(Y) = -f(-Y). \tag{18}$$

By using the center manifold theory [7], Eq. (16) can be reduced to a three-dimensional system on the center manifold, that is [8]

$$\mathrm{d}y_c/\mathrm{d}\tau = (J_c + \bar{A}_{c1})y_c + f_c(y_c, 0) + \mathrm{O}(|\delta|^2|y_c| + |\delta||y_c|^3 + |y_c|^5). \tag{19}$$

Here $\bar{A}_{c1}$ is a 3×3 matrix which is dependent on the parameter δ. The elements of $\bar{A}_{c1}$ are given as follows:

$$C_{mn} = u_{m3}\sum_{i=1}^{4} \bar{a}_i v_{in} + u_{m4}\sum_{i=1}^{4} \bar{b}_i v_{in} \quad (m = 1, 2, 3,\ n = 1, 2, 3), \tag{20}$$

where

$$\bar{a}_1 = -(2u_0c_{11}\delta_1 + g_{11}\delta_2), \quad \bar{a}_2 = -(2u_0c_{12}\delta_1 + g_{12}\delta_2),$$
$$\bar{a}_3 = -2\sqrt{\beta}b_{11}\delta_1, \qquad \bar{a}_4 = -2\sqrt{\beta}b_{12}\delta_1,$$
$$\bar{b}_1 = -(2u_0c_{21}\delta_1 + g_{21}\delta_2), \qquad \bar{b}_2 = -(2u_0c_{22}\delta_1 + g_{22}\delta_2),$$
$$\bar{b}_3 = -2\sqrt{\beta}b_{21}\delta_1, \qquad \bar{b}_4 = -2\sqrt{\beta}b_{22}\delta_1. \tag{21}$$

Here v_{ij} and u_{ij} are the elements of matrix V and V^{-1}, respectively.

In order to investigate the unfolding of Eq. (19), next, we will further reduce Eq. (19) to a normal form by using Birkhoff's normal form theory [8]. Since only the case of $|\delta| \ll 1$ is considered here, the matrix $J_c + \bar{A}_{c1}$ possesses the eigenvalues of the form given by

$$\upsilon_1 = \zeta_2(\delta), \qquad \upsilon_2 = \zeta_1(\delta) + \mathrm{i}\omega_1(\delta),$$
$$\upsilon_3 = \zeta_1(\delta) - \mathrm{i}\omega_1(\delta) = \bar{\upsilon}_2, \qquad \zeta_1, \zeta_2, \omega_1 \in \mathbb{R}. \tag{22}$$

Note that, when $\delta \to 0$ we have $\zeta_1(\delta), \zeta_2(\delta) \to 0$ and $\omega_1(\delta) \to \omega_0$.

Let $v, w, \bar{w}$ and $v^*, \bar{w}^*, w^*$ denote the normalized and their adjoint eigenvectors of the matrix $J_c + \bar{A}_{c1}$ corresponding to the eigenvalues of $\upsilon_1, \upsilon_2, \upsilon_3$, respectively. Introducing a transformation

$$y_c = zv + sw + \overline{sw}, \qquad z \in \mathbb{R},\ s \in \mathbb{C}, \tag{23}$$

Eq. (19) becomes

$$v\frac{\mathrm{d}z}{\mathrm{d}\tau}+w\frac{\mathrm{d}s}{\mathrm{d}\tau}+\bar{w}\frac{\mathrm{d}\bar{s}}{\mathrm{d}\tau}=\upsilon_1 vz+\upsilon_2 ws+\upsilon_3\overline{ws}+N(z,s,\bar{s}), \tag{24a}$$

where

$$N(z,s,\bar{s})=f_c(zv+sw+\overline{sw},0). \tag{24b}$$

Since the non-linear terms in f_c are all cubic with respect to y_c, the non-linear function N can be written as

$$N(z,s,\bar{s})=\sum z^m s^n \bar{s}^p a_{mnp}\,, \qquad a_{mnp}\in\mathbb{C}\,, \tag{25}$$

where m,n,p are non-negative integers, and the summation $\sum$ is always performed for $m+n+p=3$. Next we form the inner products of Eq. (24a) with v^* and w^* to obtain

$$\begin{aligned}\frac{\mathrm{d}z}{\mathrm{d}\tau}&=\upsilon_1 z+\sum z^m s^n \bar{s}^p d^{(1)}_{mnp},\\ \frac{\mathrm{d}s}{\mathrm{d}\tau}&=\upsilon_2 s+\sum z^m s^n \bar{s}^p d^{(2)}_{mnp},\end{aligned} \tag{26}$$

where

$$\begin{aligned}d^{(1)}_{mnp}&=<a_{mnp},v^*>=\frac{1}{2\pi}\int_0^{2\pi} a_{mnp}v^*\mathrm{d}\tau,\\ d^{(2)}_{mnp}&=<a_{mnp},w^*>=\frac{1}{2\pi}\int_0^{2\pi} a_{mnp}w^*\mathrm{d}\tau.\end{aligned} \tag{27}$$

Now we introduce a non-linear transformation of variables

$$\tilde{z}=z+\sum \alpha_{mnp}\, z^m s^n \bar{s}^p, \qquad \tilde{s}=s+\sum \beta_{mnp}\, z^m s^n \bar{s}^p. \tag{28}$$

Then we can remove, through appropriate choices of α_{mnp} and β_{mnp} in Eqs. (28), from Eqs. (26) some non-linear terms which have no influence on the topological structure of the solutions, and one can finally obtain the following normal form Eqs. [8]:

$$\begin{aligned}\frac{\mathrm{d}\tilde{z}}{\mathrm{d}\tau}&=\upsilon_1\tilde{z}+\tilde{z}|\tilde{s}|^2 d^{(1)}_{111}+\tilde{z}^3 d^{(1)}_{300},\\ \frac{\mathrm{d}\tilde{s}}{\mathrm{d}\tau}&=\upsilon_2\tilde{s}+\tilde{s}|\tilde{s}|^2 d^{(2)}_{021}+\tilde{z}^2\tilde{s} d^{(2)}_{210}.\end{aligned} \tag{29a}$$

This implies that the solutions of Eqs. (26) have the same topological structure with those of Eqs. (29a) in the local domain [8]. Therefore, removing all the non-linear terms from Eqs. (26) except the terms of $z|s|^2$ and z^3 in the first equation and the terms of $s^2 s$ and $z^2 s$ in the second will have no influences on the qualitative features of solutions of the system. The normal form equation (29a) can be exchanged to an alternative form by introducing cylindrical co-ordinate

$$\tilde{s}=\tilde{\rho}\mathrm{e}^{\mathrm{i}\varphi} \quad (\tilde{\rho}\neq 0), \tag{29b}$$

That is,

$$\begin{aligned}\frac{\mathrm{d}\tilde{\rho}}{\mathrm{d}\tau} &= \zeta_1\tilde{\rho} + S_R\tilde{\rho}^3 + Z_R\tilde{z}^2\tilde{\rho},\\ \frac{\mathrm{d}\varphi}{\mathrm{d}\tau} &= \omega_1 + S_I\tilde{\rho}^2 + Z_I\tilde{z}^2,\\ \frac{\mathrm{d}\tilde{z}}{\mathrm{d}\tau} &= \zeta_2\tilde{z} + d^{(1)}_{111}\tilde{z}\tilde{\rho}^2 + d^{(1)}_{300}\tilde{z}^3,\end{aligned} \tag{30}$$

where

$$\begin{aligned}S_R &= R_e(d^{(2)}_{021}), \qquad S_I = I_m(d^{(2)}_{021}),\\ Z_R &= R_e(d^{(2)}_{210}), \qquad Z_I = I_m(d^{(2)}_{210}).\end{aligned} \tag{31}$$

The first and third of equations (30) are independent on variable φ which represents the phase component of the solution, so the second one which involves the variable φ can be ignored here. Let

$$\rho = \sqrt{|S_R|}\,\tilde{\rho}, \quad z' = \sqrt{\left|d^{(1)}_{300}\right|}\,\tilde{z}, \tag{32}$$

then the first and third of equations (30) become

$$\begin{aligned}\frac{\mathrm{d}\rho}{\mathrm{d}\tau} &= \rho(\zeta_1 + \bar{\gamma}\rho^2 + \eta z^2),\\ \frac{\mathrm{d}z}{\mathrm{d}\tau} &= z(\zeta_2 + \theta\rho^2 + \bar{\varepsilon}z^2),\end{aligned} \tag{33a}$$

where

$$\bar{\gamma} = S_R/|S_R| = \pm 1 \qquad \eta = Z_R/\left|d^{(1)}_{300}\right|, \qquad \bar{\varepsilon} = d^{(1)}_{300}/\left|d^{(1)}_{300}\right| = \pm 1, \qquad \theta = d^{(1)}_{111}/|S_R|. \tag{33b}$$

Here we have rewritten z' as z for simplicity.

4. Calculation of the coefficients in the normal form equations

In the preceding section, we have derived the normal form equations of the system near the doubly degenerate equilibrium. To unfold the degeneracy we need to compute all the coefficients of non-linear terms in the normal form equations (33a), which are in a form of the formal equations at this stage. To determine the expressions of the coefficients $\bar{\gamma}$, η, $\bar{\varepsilon}$ and θ, we need to make a number of transformations from the original equations as indicated in the preceding section. This procedure is quite complicated, and it is hard to give the explicit formulation for the expressions.

The purpose of this section is to acquaint the reader with the details of the procedure and steps, that may be unfamiliar to some readers, for calculation of the coefficients from the original parameters of the system, and allows the reader, who so desires, to apply the technique to the similar bifurcation problem in any other physical and engineering systems.

Let us start with Eq. (14). At first we need to make some preparations for carrying out several transformations later. Solving Eqs. (8) and (9) for u and k_1, and then substituting them into Eq. (5), one may construct the matrix A_{μ_0}. Next we need to solve two eigenvalue problems of 4×4 matrix A_{μ_0} and 3×3 matrix $J_c+\bar{A}_{c1}$. Using the eigenvectors of A_{μ_0} we can compose the transformation matrix V that may put A_{μ_0} into Jordan normal form. Let

$$V=[V_1\vdots V_2],\quad V^{-1}=\begin{bmatrix}U_{11} & U_{12}\\ U_{21} & U_{22}\end{bmatrix}. \tag{34}$$

Here V_1, V_2, U_{11}, U_{12}, U_{21} and U_{22} are 4×3, 4×1, 3×2, 3×2, 1×2 and 1×2 partitioned matrices, respectively. The eigenvalues $\upsilon_1,\upsilon_2,\upsilon_3$ of the matrix $J_c+\bar{A}_{c1}$ are expressed in Eqs. (22). Let $v_i,w_i,\bar{w}_i$ and $v_i^*,\bar{w}_i^*,w_i^*$ $(i=1,2,3)$ be the elements of the vectors $v,w,\bar{w}$ and $v^*,\bar{w}^*,w^*$, respectively, which denote the normalized and their adjoint eigenvectors of the matrix $J_c+\bar{A}_{c1}$ corresponding to the eigenvalues $\upsilon_1,\upsilon_2,\upsilon_3$, respectively.

In the following, our attention will be focused on the transformations of the non-linear term $F(X)$ in Eq. (14). Let

$$F(X)=(\bar{0},\bar{F})^{\mathrm{T}},$$

where

$$\bar{0}=(0,0)^{\mathrm{T}},\qquad \bar{F}=(F_3,F_4)^{\mathrm{T}}. \tag{35}$$

Then, the non-linear term $f(Y)$ in Eqs. (17) can be written as

$$f(Y)=V^{-1}F(VY)=\begin{bmatrix}U_{11} & U_{12}\\ U_{21} & U_{22}\end{bmatrix}\begin{pmatrix}\bar{0}\\ \bar{F}([V_1\vdots V_2](y_c,y_d)^{\mathrm{T}})\end{pmatrix}\equiv\begin{pmatrix}f_c(Y)\\ f_d(Y)\end{pmatrix}. \tag{36}$$

Here $f_c(Y)$ is the non-linear term in equation on the center manifold and may be written as

$$f_c(Y)=U_{12}\bar{F}([V_1\vdots V_2](y_c,y_d)^{\mathrm{T}})=U_{12}\bar{F}(V_1y_c+V_2y_d)\equiv f_c(y_c,y_d). \tag{37}$$

Since $\bar{F}(X)$ is the homogeneous cubic polynomial of x_i and the center manifold $y_d=h(y_c)$ is at least quadratic in y_c, the non-linear term $f_c(Y)$ on the center manifold can be simplified as $f_c(y_c,0)$ by setting $y_d=0$ if we only require to consider non-linear terms up to order 3 in the normal form equations:

$$f_c(y_c,0)=U_{12}\bar{F}(V_1y_c)=U_{12}\begin{pmatrix}F_3(V_1y_c)\\ F_4(V_1y_c)\end{pmatrix}. \tag{38}$$

This means that to obtain the equation on the center manifold with non-linear terms up to order 3 we need only to make the transformation

$$X=V_1y_c \tag{39}$$

for non-linear terms in Eq. (14), not transformation (15). If we substitute Eq. (23) into Eq. (39) to combine the two transformations, we may obtain

$$X=fz+gs+\overline{gs} \tag{40}$$

or

$$x_i=f_iz+g_is+\overline{g_is}\quad(i=1,\ldots,4), \tag{41}$$

where

$$f=(f_1,f_2,f_3,f_4)^{\mathrm{T}}=V_1v,\qquad f_i=\sum_{j=1}^{3}v_{ij}\,v_j,$$

$$g=(g_1,g_2,g_3,g_4)^{\mathrm{T}}=V_1w,\qquad g_i=\sum_{j=1}^{3}v_{ij}\,w_j,$$

$$\bar{g}=(\bar{g}_1,\bar{g}_2,\bar{g}_3,\bar{g}_4)^{\mathrm{T}}=V_1\bar{w},\qquad \bar{g}_i=\sum_{j=1}^{3}v_{ij}\,\bar{w}_j,\qquad (i=1,\ldots,4). \tag{42}$$

Let R_i and I_i be the real and imaginary parts of g_i, respectively. That is,

$$R_i=R_e(g_i),\qquad I_i=I_m(g_i),$$
$$g_i=R_i+\mathrm{i}I_i,\qquad \bar{g}_i=R_i-\mathrm{i}I_i\qquad (i=1,\ldots,4), \tag{43a}$$

where

$$R_i=\sum_{j=1}^{3}v_{ij}\,w_{jR},\qquad I_i=\sum_{j=1}^{3}v_{ij}\,w_{jI},$$
$$\mathrm{i}=\sqrt{-1},\qquad w_{iR}=R_e(w_i),\qquad w_{iI}=I_m(w_i),$$
$$w_i=w_{iR}+\mathrm{i}w_{iI}\qquad (i=1,\ldots,4). \tag{43b}$$

Substituting Eq. (40) or (41) into the expressions of F_3 and F_4 [6] in Eq. (14), we may obtain the new expressions of F_3 and F_4 as functions of the new variables z, s and $\bar{s}$:

$$F_3=\gamma_1z^3+\gamma_2z^2s+\gamma_3z|s|^2+\gamma_4s|s|^2+\cdots,$$
$$F_4=\varepsilon_1z^3+\varepsilon_2z^2s+\varepsilon_3z|s|^2+\varepsilon_4s|s|^2+\cdots, \tag{44}$$

where

$$\gamma_1=-k_2\varphi_1(\xi_b)\varphi_f^3,\quad \gamma_2\equiv\gamma_{2R}+\mathrm{i}\gamma_{2I},\quad \gamma_{2R}=-3k_2\varphi_1(\xi_b)\varphi_f^2\varphi_R,\quad \gamma_{2I}=-3k_2\varphi_1(\xi_b)\varphi_f^2\varphi_I,$$
$$\gamma_3=-6k_2\varphi_1(\xi_b)\varphi_f(\varphi_R^2+\varphi_I^2),\quad \gamma_4\equiv\gamma_{4R}+\mathrm{i}\gamma_{4I},$$
$$\gamma_{4R}=-3k_2\varphi_1(\xi_b)(\varphi_R^2+\varphi_I^2)\varphi_R,\quad \gamma_{4I}=-3k_2\varphi_1(\xi_b)(\varphi_R^2+\varphi_I^2)\varphi_I,$$
$$\varphi_f=\sum_{i=1}^{2}\varphi_i(\xi_b)f_i,\quad \varphi_R=\sum_{i=1}^{2}\varphi_i(\xi_b)R_i,\quad \varphi_I=\sum_{i=1}^{2}\varphi_i(\xi_b)I_i,$$
$$\varepsilon_1=\gamma_1/e,\quad \varepsilon_2\equiv\varepsilon_{2R}+\mathrm{i}\varepsilon_{2I},\quad \varepsilon_{2R}=\gamma_{2R}/e,\quad \varepsilon_{2I}=\gamma_{2I}/e,$$
$$\varepsilon_3=\gamma_3/e,\quad \varepsilon_4\equiv\varepsilon_{4R}+\mathrm{i}\varepsilon_{4I},\quad \varepsilon_{4R}=\gamma_{4R}/e,\quad \varepsilon_{4I}=\gamma_{4I}/e,$$
$$e=\varphi_1(\xi_b)/\varphi_2(\xi_b). \tag{45}$$

Note that, since in the normal form equations, Eqs. (29a), there are only non-linear terms of z^3, z^2s, $z|s|^2$ and $s|s|^2$ we do not need to compute any non-linear term except those containing these four cubic terms in the expressions of F_3 and F_4 in Eq. (44). Substituting Eqs. (23) and (44) into

Eqs. (38) and using Eq. (24b), we obtain

$$N_i(z,s,\bar{s}) = a_{300}^{(i)} z^3 + a_{210}^{(i)} z^2 s + a_{111}^{(i)} z|s|^2 + a_{021}^{(i)} s|s|^2 + \cdots \quad (i = 1,2,3). \tag{46}$$

Here $a_{300}^{(i)}$, $a_{210}^{(i)}$, $a_{11}^{(i)}$ and $a_{021}^{(i)}$ ($i = 1, 2, 3$) denote the elements of the vectors a_{300}, a_{210}, a_{111} and a_{021}, respectively, and

$$\begin{aligned}
&(N_1, N_2, N_3)^{\mathrm{T}} = N, \quad a_{300}^{(i)} = u_{i3}\gamma_1 + u_{i4}\varepsilon_1,\\
&a_{210}^{(i)} = u_{i3}\gamma_2 + u_{i4}\varepsilon_2 = u_{i3}\gamma_{2R} + u_{i4}\varepsilon_{2R} + \mathrm{i}(u_{i3}\gamma_{2I} + u_{i4}\varepsilon_{2I}),\\
&a_{111}^{(i)} = u_{i3}\gamma_3 + u_{i4}\varepsilon_3,\\
&a_{021}^{(i)} = u_{i3}\gamma_4 + u_{i4}\varepsilon_4 = u_{i3}\gamma_{4R} + u_{i4}\varepsilon_{4R} + \mathrm{i}(u_{i3}\gamma_{4I} + u_{i4}\varepsilon_{4I}) \quad (i = 1,2,3).
\end{aligned} \tag{47}$$

If we substitute Eqs. (47) into Eqs. (27), we may obtain the coefficients of non-linear terms in the normal form equations (29a):

$$\begin{aligned}
d_{111}^{(1)} &= \langle a_{111}, v^* \rangle = \sum_{i=1}^{3} a_{111}^{(i)} v_i^* = \sum_{i=1}^{3} (u_{i3}\gamma_3 + u_{i4}\varepsilon_3) v_i^*,\\
d_{300}^{(1)} &= \langle a_{300}, v^* \rangle = \sum_{i=1}^{3} a_{300}^{(i)} v_i^* = \sum_{i=1}^{3} (u_{i3}\gamma_1 + u_{i4}\varepsilon_1) v_i^*,\\
d_{021}^{(2)} &= \langle a_{021}, w^* \rangle = \sum_{i=1}^{3} a_{021}^{(i)} w_i^* = \sum_{i=1}^{3} [u_{i3}\gamma_{4R} + u_{i4}\varepsilon_{4R} + \mathrm{i}(u_{i3}\gamma_{4I} + u_{i4}\varepsilon_{4I})](w_{iR}^* + \mathrm{i}w_{iI}^*) \equiv S_R + \mathrm{i}S_I,\\
S_R &= R_e(d_{021}^{(2)}) = \sum_{i=1}^{3} [u_{i3}\gamma_{4R} + u_{i4}\varepsilon_{4R}) w_{iR}^* - (u_{i3}\gamma_{4I} + u_{i4}\varepsilon_{4I}) w_{iI}^*]\\
S_I &= I_m(d_{021}^{(2)}) = \sum_{i=1}^{3} [u_{i3}\gamma_{4R} + u_{i4}\varepsilon_{4R}) w_{iI}^* + (u_{i3}\gamma_{4I} + u_{i4}\varepsilon_{4I}) w_{iR}^*]\\
d_{210}^{(2)} &= \langle a_{210}, w^* \rangle = \sum_{i=1}^{3} a_{210}^{(i)} w_i^* = \sum_{i=1}^{3} [u_{i3}\gamma_{2R} + u_{i4}\varepsilon_{2R} + \mathrm{i}(u_{i3}\gamma_{2I} + u_{i4}\varepsilon_{2I})](w_{iR}^* + \mathrm{i}w_{iI}^*) \equiv Z_R + \mathrm{i}Z_I,\\
Z_R &= R_e(d_{210}^{(2)}) = \sum_{i=1}^{3} [u_{i3}\gamma_{2R} + u_{i4}\varepsilon_{2R}) w_{iR}^* - (u_{i3}\gamma_{2I} + u_{i4}\varepsilon_{2I}) w_{iI}^*],\\
Z_I &= I_m(d_{210}^{(2)}) = \sum_{i=1}^{3} [u_{i3}\gamma_{2R} + u_{i4}\varepsilon_{2R}) w_{iI}^* + (u_{i3}\gamma_{2I} + u_{i4}\varepsilon_{2I}) w_{iR}^*],
\end{aligned} \tag{48}$$

where

$$w_{iR}^* = R_e(w_i^*), \qquad w_{iI}^* = I_m(w_i^*).$$

Substituting Eqs. (48) into Eqs. (33b), we finally obtain the expressions of the coefficients $\bar{\gamma}$, η, $\bar{\varepsilon}$ and θ in Eqs. (33a).

5. Local bifurcations

We now investigate the bifurcations of solution of the system through analyzing the reduced Eqs. (33a) which should possess all information about local behavior of the original four-dimensional system except the phase effect [8, 9].

Obviously, the coefficients $\bar{\gamma}, \eta, \bar{\varepsilon}, \theta$ in Eqs. (33a) all depend on the parameters α and β. Numerical analysis shows that for the values of α and β that fulfill the conditions (8) and (9) we have $\bar{\gamma} = -1, \eta < 0, \bar{\varepsilon} = 1$ and $\theta > 0$. Therefore, Eq. (33a) can be written as

$$\begin{aligned} \frac{\mathrm{d}\rho}{\mathrm{d}\tau} &= \rho(\zeta_1 - \rho^2 + \eta z^2), \\ \frac{\mathrm{d}z}{\mathrm{d}\tau} &= z(\zeta_2 + \theta\rho^2 + z^2), \end{aligned} \tag{49}$$

where $\eta < 0$ and $\theta > 0$. The system of Eqs. (49) has been encountered in many physical problems [10,11] and investigated from various aspect for their different special purpose of problem. Here we first briefly summarize some basic results for our purpose. To unfold the bifurcations of Eqs. (49) one first needs to determine the equilibria and their stability. Because of the symmetry with respect to both axes of ρ and z in Eqs. (49), in what follows, the equilibria and phase portraits are only illustrated in the first quadrant. The equilibria are given by

$$\rho(\zeta_1 - \rho^2 + \eta z^2) = 0, \qquad z(\zeta_2 + \theta\rho^2 + z^2) = 0. \tag{50}$$

Obviously, there are four equilibria, as follows

$$\begin{aligned} &(1)\ (\rho, z) = (0, 0); \\ &(2)\ (\rho, z) = (\sqrt{\zeta_1}, 0) \text{ for } \zeta_1 > 0; \\ &(3)\ (\rho, z) = (0, \sqrt{-\zeta_2}), \text{ for } \zeta_2 > 0; \\ &(4)\ (\rho, z) = (\sqrt{(\zeta_1 - \eta\zeta_2)/(1 + \theta\eta)}, \sqrt{-(\theta\zeta_1 + \zeta_2)/(1 + \theta\eta)}) \\ &\quad \text{for } \zeta_2 < \zeta_1/\eta \text{ and } \zeta_2 < -\theta\zeta_1 \text{ if } 0 < \theta < -1/\eta, \\ &\quad \text{or, for } \zeta_2 > \zeta_1/\eta \text{ and } \zeta_2 > -\theta\zeta_1 \text{ if } \theta > -1/\eta \end{aligned} \tag{51}$$

The stability of the equilibria and flow behavior near these equilibria can be determined by the eigenvalues of the Jacobi matrix of the right side in Eqs. (49). The Jacobi matrix has the general form

$$J_0 = \begin{bmatrix} \zeta_1 - 3\rho^2 + \eta z^2 & 2\eta\rho z \\ 2\theta\rho z & \zeta_2 + \theta\rho^2 + 3z^2 \end{bmatrix},$$

and we may evaluate the matrix at every equilibrium, as follows:

$$J_1 = \begin{bmatrix} \zeta_1 & 0 \\ 0 & \zeta_2 \end{bmatrix}, \qquad J_2 = \begin{bmatrix} -2\zeta_1 & 0 \\ 0 & \zeta_2 + \theta\zeta_1 \end{bmatrix}, \qquad J_3 = \begin{bmatrix} \zeta_1 - \eta\zeta_2 & 0 \\ 0 & -2\zeta_2 \end{bmatrix},$$

$$J_4 = \begin{bmatrix} -2(\zeta_1 - \eta\zeta_2)/(1 + \theta\eta) & 2\eta\sqrt{-(\zeta_1 - \eta\zeta_2)(\theta\zeta_1 + \zeta_2)/(1 + \theta\eta)^2} \\ 2\theta\sqrt{-(\zeta_1 - \eta\zeta_2)(\theta\zeta_1 + \zeta_2)/(1 + \theta\eta)^2} & -2(\theta\zeta_1 + \zeta_2)/(1 + \theta\eta) \end{bmatrix}, \tag{52}$$

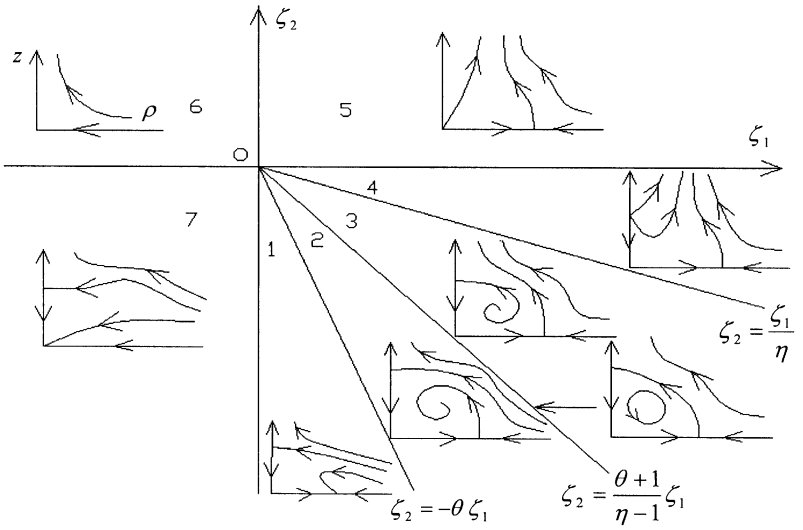

Fig. 3. Bifurcation set and phase portraits of Eqs. (49).

where J_1 to J_4 represent the Jacobi matrices evaluated at equilibria (1)–(4), respectively. Thus, it is easy to show from expressions (52) that primary pitchfork bifurcations occur from the trivial equilibrium (1) on the lines $\zeta_1 = 0$ and $\zeta_2 = 0$, and we obtain non-trivial equilibriums (2) for $\zeta_1 > 0$ and (3) for $\zeta_2 < 0$. Secondary pitchfork bifurcations can also occur from equilibrium (2) on the line $\zeta_2 + \theta\zeta_1 = 0$, and from (3) on the line $\zeta_1 - \eta\zeta_2 = 0$, and we obtain the equilibrium (4). The bifurcation set in the ζ_1–ζ_2 plane and the corresponding phase portraits of Eqs. (49) in each region are given in Fig. 3.

The same unfolding result for Eqs. (49) may be obtained from a different way. We introduce the following transformations:

$$\tau \to -\tau, \qquad \zeta_1 \to -\zeta_1, \qquad \zeta_2 \to -\zeta_2, \tag{53}$$

then Eqs. (49) become

$$\begin{aligned} \frac{\mathrm{d}\rho}{\mathrm{d}\tau} &= \rho(\zeta_1 + \rho^2 - \eta z^2), \\ \frac{\mathrm{d}z}{\mathrm{d}\tau} &= z(\zeta_2 - \theta\rho^2 - z^2). \end{aligned} \tag{54}$$

The unfoldings for Eqs. (54) have been investigated in Ref. [9]. The relation between the coefficients in Eqs. (54) and the corresponding Eqs. (7.5.2) studied in Ref. [9] is given as follows:

$$\begin{aligned} &-\eta \leftrightarrow b, \qquad -\theta \leftrightarrow c, \qquad -1 \leftrightarrow d, \\ &-1-(-\eta)(-\theta) = -1-\eta\theta \leftrightarrow d - bc = v. \end{aligned} \tag{55}$$

Because of $\eta < 0, \theta > 0$, we have

$$b > 0, \quad c < 0, \quad v > 0, \tag{56}$$

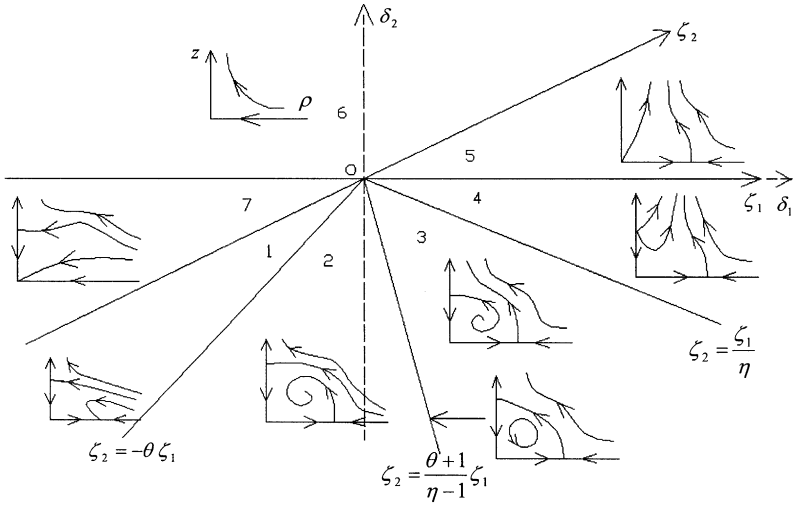

Fig. 4. Bifurcation set and phase portraits in the δ_1–δ_2 plane.

and so Eqs. (54) indeed correspond to the case VIa in Ref. [9]. The unfolding result of Fig. 3 for Eqs. (49) then can be easily obtained also from Figure (7.5.5) in Ref. [9] if we take into account transformations (53).

Since $\zeta_1(\delta)$ and $\zeta_2(\delta)$ may be regarded as the linear functions of $\delta = (\delta_1, \delta_2)$ when $\delta \to 0$, it is easy to determine numerically the axes of ζ_1 and ζ_2 and the bifurcation set mentioned above in the δ_1–δ_2 parameter plane. Fig. 4 shows the bifurcation set and phase portraits for Eqs. (49), which are drown in the δ_1–δ_2 plane.

There is an interesting problem about the possibility that Hopf bifurcations occur from the equilibrium (4). Hopf bifurcations will occur in the system of Eqs. (49) or (54) if the trace of the Jacobi matrix J_4 becomes zero, that is

$$tr(J_4) = \frac{-2\zeta_1(1+\theta) + 2\zeta_2(\eta-1)}{1+\theta\eta} = 0, \tag{57}$$

which gives

$$-\zeta_1(1+\theta) + \zeta_2(\eta-1) = 0, \quad \text{or} \quad \zeta_2 = \frac{1+\theta}{\eta-1}\zeta_1. \tag{58}$$

However, one can show that the Hopf bifurcation on the line of $\zeta_2 = (1+\theta)\zeta_1/(\eta-1)$ is degenerate [9], and thus the stability computations of the bifurcation cannot be carried out at this stage to obtain specific criteria for sub- or super-critical bifurcations. Therefore, the higher-order terms in the center manifold and induced by the non-linear transformation of Eq. (28) should be added to our normal form Eqs. (49) to determine the topological type of solution of the system near the line. The unfolding computations for this case are very complicated. We need, firstly, find a rescaling that transformed the normal form equations into a perturbation of an integrable Hamiltonian system with the higher order terms added in the normal form part of the perturbation. Then the Melnikov theory can be used to analyze the dependence of periodic orbits

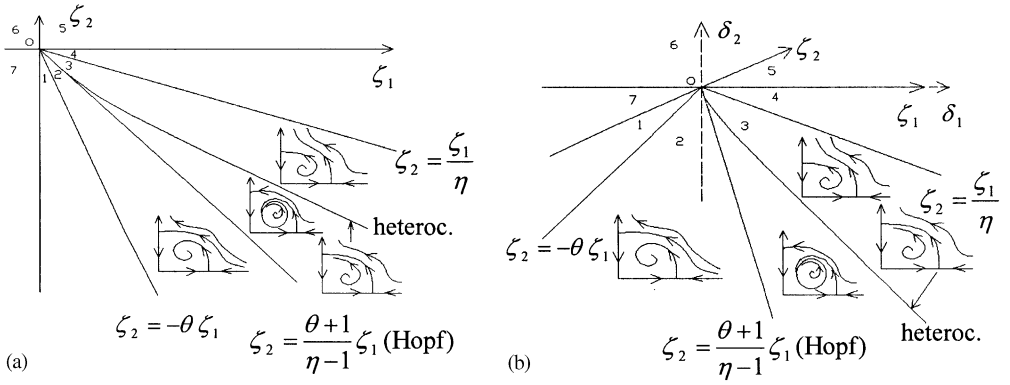

Fig. 5. (a) A completion of the unfolding shown in Fig. 3; (b) A completion of the unfolding shown in Fig. 4.

on the parameters and find the bifurcation curve for heteroclinic loop. Regarding this kind of analysis and calculations, the reader can consult Ref. [9] for the analysis of a special case, $\eta = -3$ and $\theta = 3$, of Eqs. (54). However, it is too hard to carry out the unfolding computations for the present problem, especially using the original physical parameters, so we only conjecture here for this system that a stable limit cycle around equilibrium (4) will be born through a supercritical Hopf bifurcation from equilibrium (4) on the line of $\zeta_2 = (1+\theta)\zeta_1/(\eta-1)$. The completions of the unfoldings shown in Figs. 3 and 4 are sketched in Fig. 5 on the basis of the conjecture. We will confirm the conjecture and the results shown in Fig. 4 in the next section through carrying out numerical simulations by solving Eq. (6) directly.

Finally, in order to provide a physical interpretation of the results shown in Figs. 4 and 5, we turn to a brief discussion regarding the relationship between the dynamics of the reduced plane autonomous system, Eqs. (49), and the discretized four-dimensional system, Eq. (6). One should reconsider the rotational effect, the second of Eqs. (30), neglected at a stage in the analysis to complete the analysis and explain the results obtained. It is easy to see that the following correspondences exist:

Planar system Four-dimensional system

(1) $(z,\rho) = (0,0)$ → undeformed state of the pipe.
(2) $(z,\rho) = (\bar{z},0)$ → buckled state of the pipe.
(3) $(z,\rho) = (0,\bar{\rho})$ → periodic motions encircling the zero equilibrium.
(4) $(z,\rho) = (\bar{z},\bar{\rho})$ → periodic motions encircling the non-zero equilibriums.
(5) Periodic orbit (limit cycle) → two-dimensional torus, quasi-periodic motions,

where $\bar{z}$ and $\bar{\rho}$ represent the values of z and ρ at the fixed points in Figs. 3 (and 4), respectively. It is easy to imagine that the limit cycle motion around equilibrium (4) in the reduced planar system may be regarded as a motion on the surface of two-dimensional torus in the three- or four-dimensional state space if we take into account the rotational effect neglected. A sketch illustrating the motion on the surface of two-dimensional torus is shown in Fig. 6. This motion itself is not periodic but is said to be quasi-periodic or almost-periodic.

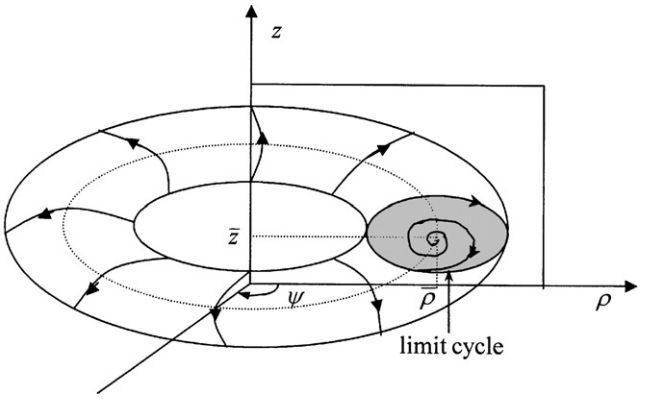

Fig. 6. Sketch illustrating the motion on the surface of two-dimensional torus.

6. Numerical simulations

Numerical simulations are carried out by solving the four-dimensional equation (6) directly with the aid of the fourth order Runge–Kutta method to confirm the analytical results shown in Fig. 4 and the conjecture in the previous section. In the computations, we set $\alpha = 0.005$ and $\beta = 0.2$ [6]. Thus the values of u and k_1 which correspond to the doubly degenerate point M can be determined as follows:

$$u_0 = 9.828245, \quad k_{10} = 59.40064.$$

Figs. 7(a)–(g) show the phase trajectories simulated directly from Eq. (6) in some specific cases, which correspond to the behavior in regions 1–7 of Fig. 4, respectively. The phase portraits in Fig. 7 are projections of solutions onto (x_1, x_3)-plane. It is easy to see that there exist the relationships between the phase portraits in Fig. 4, Fig. 7 and the sub-regions in Fig. 2 as shown in Table 1. One can see that each line of the bifurcation set in δ_1–δ_2 parameter plane shown in Fig. 4 takes almost the same direction with the boundary line of the corresponding stability region in Fig. 2 in the neighborhood of the degenerate point M. Therefore, the unfolding results shown in Fig. 4 are indeed verified except the conjecture concerning the Hopf bifurcation from equilibrium (4). In order to show that a stable limit cycle motion occurring from the Hopf bifurcation dose exist in the reduced system of Eqs. (49), one needs to confirm that a quasi-periodic motion does occur in the original four-dimensional system of Eq. (6) in the corresponding parameter range. Here, the phase portraits and Poincaré maps are used as the tools for numerical simulations, and the following two triggers are used for Poincaré maps:

(1) The state of the pipe at the point of $\xi = 0.82$ will be taken down when the velocity of the pipe at the point of $\xi = 1$ be zero, i.e.,

$$\dot{W}(1, \tau) = \varphi_1(1)\dot{q}_1(\tau) + \varphi_2(1)\dot{q}_2(\tau) = 0.$$

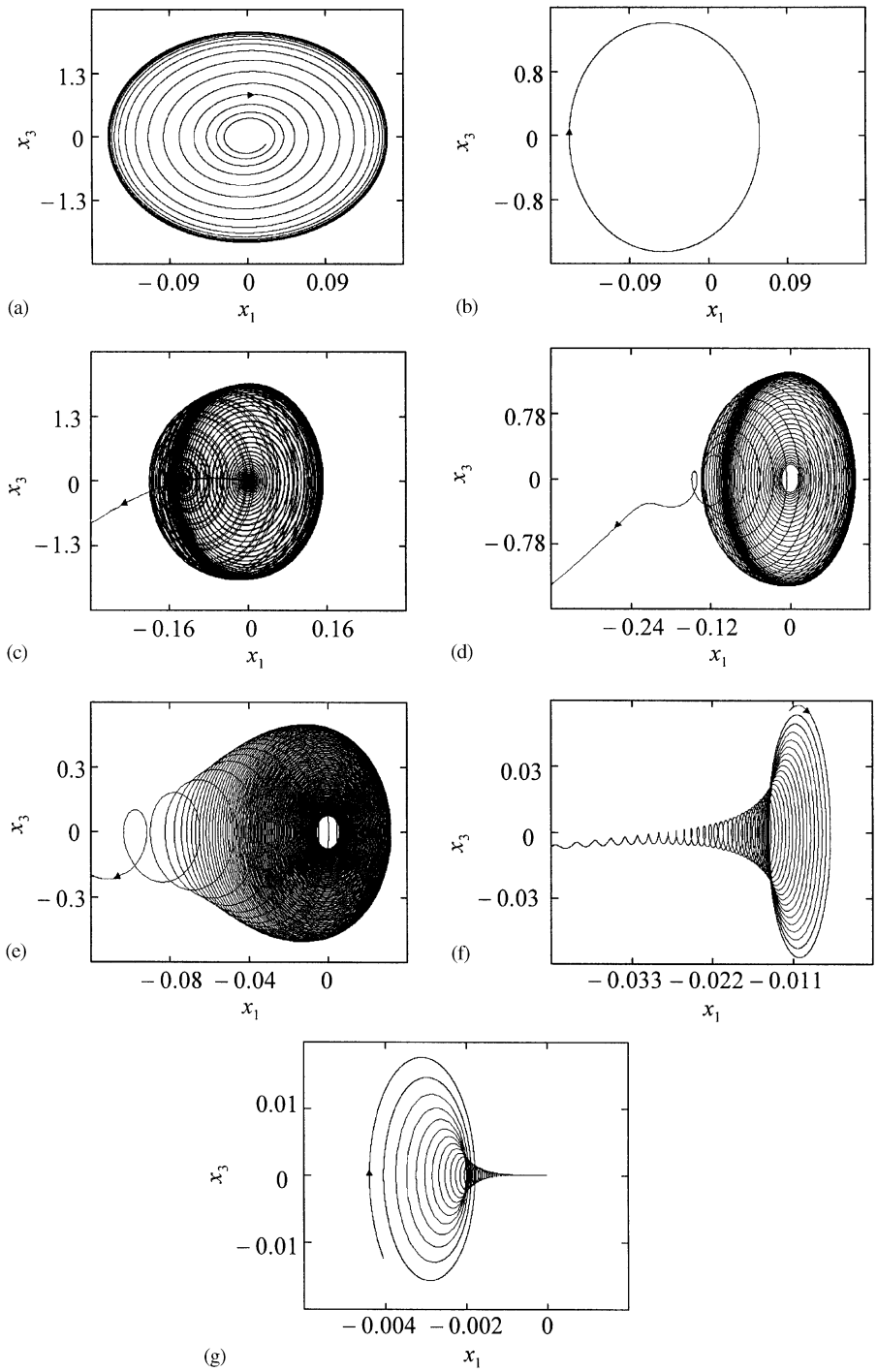

Fig. 7. Phase portraits simulated directly from Eq. (6). (a) $u=9.4$, $k_1=52$; (b) $u=9.7$, $k_1=55$; (c) $u=9.83$, $k_1=55.72$; (d) $u=9.85$, $k_1=58$; (e) $u=9.89$, $k_1=59.5$; (f) $u=9.7$, $k_1=59.5$; (g) $u=9.4$, $k_1=59.2$.

Table 1
Relationships between Figs. 2, 4 and 7

Figure 4	1	2	3	4	5	6	7
Figure 7	a	b	c	d	e	f	g
Figure 2	1	2	7	7	V	III	II

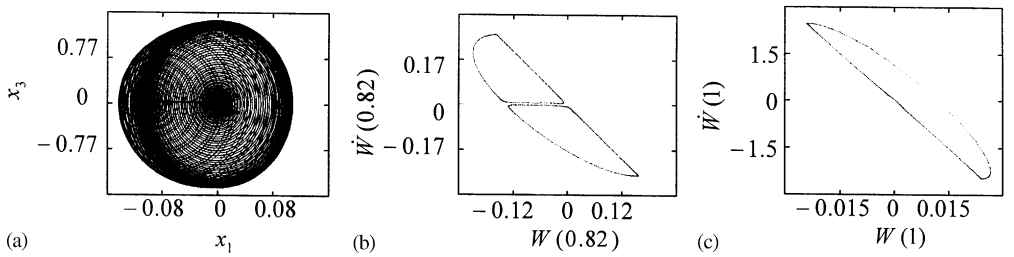

Fig. 8. A quasi-periodic motion of the system for $u = 9.82915$, $k_1 = 57.5$. (a) Phase portrait; (b) Poincaré map for trigger 1; (c) Poincaré map for trigger 2.

(2) The state of the pipe at the point of $\xi = 1$ will be taken down when the displacement of the pipe at the point of $\xi = 0.82$ be zero, i.e.,

$$W(0.82, \tau) = \varphi_1(0.82)q_1(\tau) + \varphi_2(0.82)q_2(\tau) = 0.$$

A quasi-periodic motion captured in the four-dimensional system of Eq. (6) in the corresponding parameter range near the degenerate point M is shown in Fig. 8. One can see from the figure that the Poincaré maps of the quasi-periodic motion are closed curves: double closed curves for using trigger 1 and single one for using trigger 2.

7. Conclusions and discussions

In this paper, we have studied some local stability and bifurcation problems of a cantilevered pipe conveying fluid with the motion limiting constraints and a linear spring support. The local behavior of the system in the neighborhood of a doubly degenerate point was analyzed by using some qualitative reduction methods in dynamical system theory, such as center manifold and Birkhoff's normal form theory. The analytical results obtained are found to be in good agreement with that obtained by means of numerical simulations. Furthermore, the analytical unfolding results show that the quasi-periodic motions may occur in certain parameter range in the system, which could not be detected in the early work using numerical method [6].

In addition we found that as the parameters of u and k_1 vary from the point M to the sub-region of chaotic motions (region 4) in Fig. 2 along the boundary line between the sub-regions IV and 7 chaotic motions occur as the results of the breakup of the quasi-periodic torus surface [12], as shown in Fig. 9. It is known to be a different route to chaos from that of "periodic-doubling bifurcation" which has been detected in this system earlier [3,6]. A further analysis on the

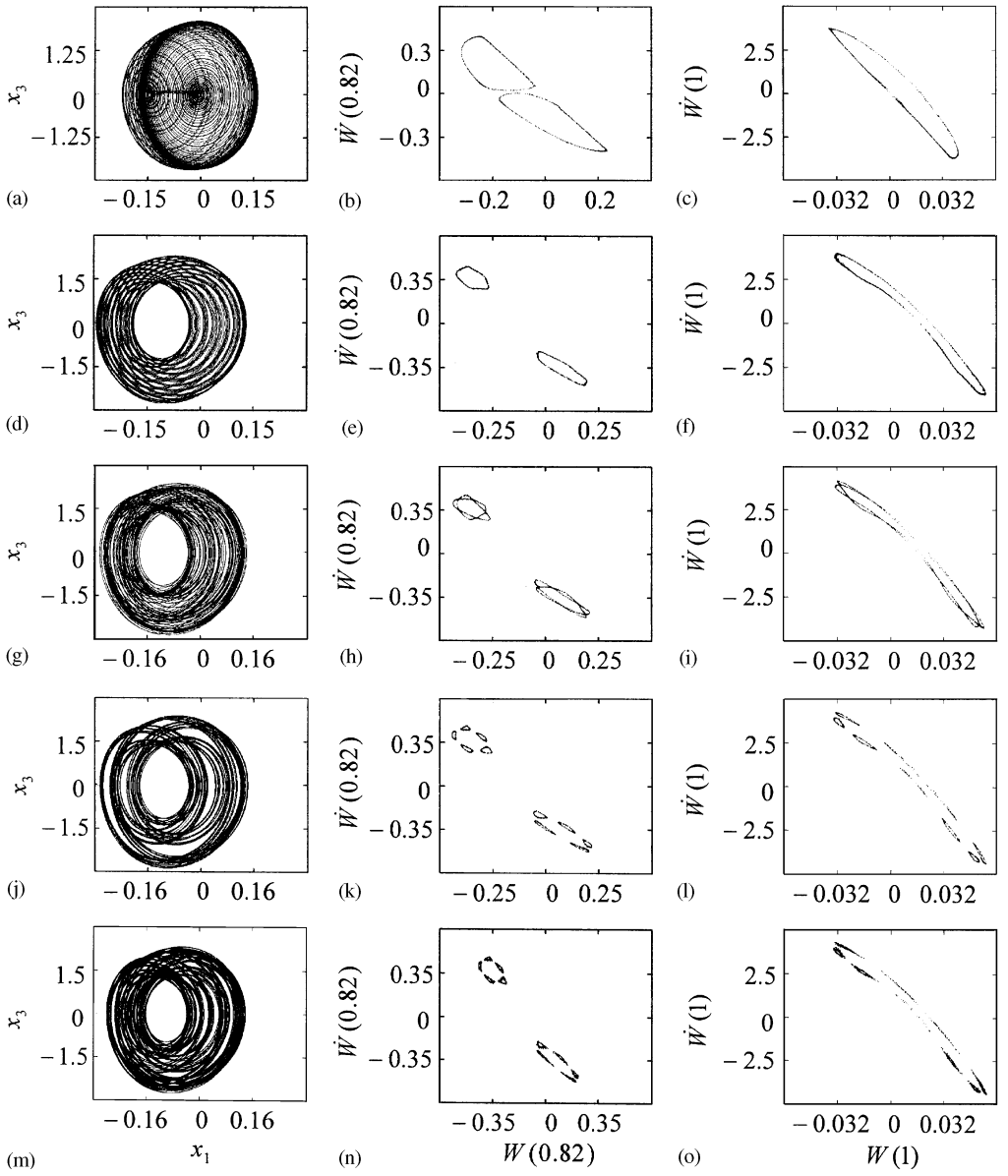

Fig. 9. Onset of chaos by breakup of the torus surface of quasi-periodic motions. (a)–(c) $u=9.8302$, $k_1=55$; (d)–(f) $u=9.832$, $k_1=50.1$; (g)–(i) $u=9.83218$, $k_1=49.8$; (j)–(l) $u=9.8322$, $k_1=49.62$; (m)–(o) $u=9.8313$, $k_1=49.6$. Where figures (a), (d), (g), (j), (m) are phase portraits, figures (b), (e), (h), (k), (n) are Poincaré maps with trigger 1, and figures (c), (f), (i), (l), (o) are Poincaré maps with trigger 2.

differences between these two kinds of chaos born from different routes, and about the ways by which one develops into the other will be published elsewhere.

Note that near the Hopf bifurcation line we may determine the line of heteroclinic orbit by the Melnikov's method as shown in Fig. 5. It gives rise to the possibility of heteroclinc tangles among

the stable and unstable manifolds of saddle loop. If this happens we may expect to find in this case a thin "wedge" around the Hopf bifurcation line in which chaotic motions occur. However, in the present system, there is a stable state with the quasi-periodic motion in that region, and so the chaotic motions would not seem to occur near the degenerate point M. Indeed, numerical simulations we carried out so far have not detected any chaotic motions in that region. The chaotic motion we detected which arises at the nearest distance from the degenerate point M ($u_0 = 9.82, k_{10} = 59.4$) is located in $k_1 = 50$, and so we do not think that it can be regarded as the chaos born from the heteroclinic tangles near the degenerate point. It should also be pointed out that based on the two-dimensional analysis we may provide merely a information about the possibility of chaotic motions in the system of four-dimensional equation. How the chaotic motions associate with the heteroclinic bifurcation are created in higher dimensional system and how the chaotic motions are created by the breakup of the quasi-periodic torus structure as the system parameter is varied are still imperfectly understood [9,13].

Appendix A. Nomenclature

$\bar{0}$	$(0,0)^{\mathrm{T}}$
a	coefficient of viscoelastic damping
a_i	element of matrix A
$\bar{a}_i$	element of matrix $A_\mu - A_{\mu 0}$
a_{mnp}	coefficient of non-linear terms
$a^{(i)}_{mnp}$	element of a_{mnp}
A	4×4 matrix, coefficients of linear part of equation of motion
A_{c1}, A_{c2}, A_{d1}, A_{d2}	3×3, 3×1, 1×3 and 1×1 partitioned submatrices of $\bar{A}_\delta$
$\bar{A}_\delta$	4×4 matrix, Eqs. (17)
A_μ	matrix A
$A_{\mu 0}$	matrix A_μ when $\mu = \mu_0$
b_i	element of matrix A
$\bar{b}_i$	element of matrix $A_\mu - A_{\mu 0}$
b_{sr}	$\int_0^1 \varphi_s(\xi)\varphi_r'(\xi)\,\mathrm{d}\xi$
c_{sr}	$\int_0^1 \varphi_s(\xi)\varphi_r''(\xi)\,\mathrm{d}\xi$
C_{mn}	element of matrix $\bar{A}_{c1}$
d_{sr}	$\int_0^1 \xi\varphi_s(\xi)\varphi_r''(\xi)\,\mathrm{d}\xi$
$d^{(i)}_{mnp}$	coefficient of non-linear terms, Eqs. (27)
D_δ	4×4 matrix, equal to A_μ
D_0	matrix D_δ when $\delta = 0$
e	$\varphi_1(\xi_b)/\varphi_2(\xi_b)$
e_{sr}	$b_{sr} + d_{sr} - c_{sr}$
EI	flexural rigidity of pipe
f	coefficient of transformation, Eq. (40)
$f(Y)$	non-linear term in equation of motion, $(f_c, f_d)^T$

$f_c,\ f_d$	non-linear terms in equation of motion, Eqs. (17)
f_i	element of f
$F,\ \bar{F},\ F_3,\ F_4$	non-linear terms in equation of motion
$g,\ \bar{g}$	coefficient of transformation, Eq. (40)
g_0	acceleration due to gravity
$g_i,\ \bar{g}_i$	element of g and $\bar{g}$, respectively
g_{sr}	$\varphi_s(\xi_b)\cdot\varphi_r(\xi_b)$
$h(\cdot)$	center manifold
H_i	coefficient of characteristic equation
i	sub- or superscript
i	$\sqrt{-1}$
I_i	imaginary part of g_i
J	4×4 matrix, Jordan normal form of $A_{\mu0}$
$J_0,\ J_1,\ J_2,\ J_3,\ J_4,$	2×2 Jacobi matrices
$S_R,\ S_I$	real and imaginary parts of $d_{021}^{(2)}$
t	time
u	non-dimensional flow velocity
u_0	value of u at degenerate point
u_{ij}	element of matrix V^{-1}
U	flow velocity
$U_{11},\ U_{12},\ U_{21},\ U_{22}$	$3\times2,\ 3\times2,\ 1\times2,\ 1\times2$ partitioned submatrices of V^{-1}
$v,\ v^*$	normalized and its adjoint eigenvectors of $J_c+\bar{A}_{c1}$ corresponding to eigenvalue of υ_1
$v_i,\ v_i^*$	elements of v and v^*, respectively
v_{ij}	elements of matrix V
V	4×4 transformation matrix
$V_1,\ V_2$	4×3 and 4×1 partitioned submatrices of V
J_c	3×3 matrix, Eq. (17)
J_d	$-H_1$
$k_1,\ k_2$	non-dimensional linear and non-linear spring constants
k_{10}	value of k_1 at degenerate point
$K_1,\ K_2$	linear and non-linear spring constants
L	length of pipe
m	mass per unit length of pipe
M	mass of fluid per unit length
N	non-linear term in equation on the center manifold
N_i	element of N
q_i	motion with ith natural mode of pipe
R_i	real part of g_i
$s,\ \bar{s},\ \tilde{s}$	variables defined in Eqs. (23) and (28)
$w,\ \bar{w},\ \bar{w}^*,\ w^*$	normalized and their adjoint eigenvectors of $J_c+\bar{A}_{c1}$ corresponding to eigenvalues of υ_2 and υ_3, respectively

w_i, w_i^*	elements of w and w^*
w_{iR}, w_{iI}	real and imaginary parts of w_i
w_{iR}^*, w_{iI}^*	real and imaginary parts of w_i^*
W	non-dimensional deflection of pipe
x	co-ordinate of pipe
x_b	location of constraint
x_i	element of X
X	variables defined in Eq. (5)
y	deflection of pipe
y_c	$(y_1, y_2, y_3)^{\mathrm{T}}$
y_d	y_4
y_i	element of Y
Y	variables defined in Eq. (15)
z, $\tilde{z}$, z'	variables defined in Eqs. (23), (28) and (32)
$\bar{z}$	the value of z at equilibrium
Z_R, Z_I	real and imaginary parts of $d_{210}^{(2)}$
α	non-dimensional coefficient of viscoelastic damping
α_{mnp}	coefficient of non-linear transformation, Eq. (28)
β	$M/(M+m)$
β_{mnp}	coefficient of non-linear transformation, Eq. (28)
γ	$(M+m)g_0L^3/(EI)$
$\bar{\gamma}$	coefficient of non-linear term in normal form equations, ± 1
γ_i	coefficient of non-linear term, Eq. (44)
γ_{2R}, γ_{2I}	real and imaginary parts of γ_2
γ_{4R}, γ_{4I}	real and imaginary parts of γ_4
δ	$(\delta_1, \delta_2)^{\mathrm{T}}$
$\delta(\cdot)$	Dirac delta function
δ_1	$u - u_0$
δ_2	$k_1 - k_{10}$
$\bar{\varepsilon}$	coefficient of non-linear term in normal form equations, ± 1
ε_i	coefficient of non-linear term, Eq. (44)
ε_{2R}, ε_{2I}	real and imaginary parts of ε_2
ε_{4R}, ε_{4I}	real and imaginary parts of ε_4
ζ_1	real part of eigenvalue υ_2
ζ_2	υ_1
θ	coefficient of non-linear term in normal form equations
η	coefficient of non-linear term in normal form equations
λ_i	ith eigenvalue of cantilevered beam
μ	$(u, k_1, \alpha, \beta)^{\mathrm{T}}$
μ_0	$(u_0, k_{10}, \alpha, \beta)^{\mathrm{T}}$
υ_i	eigenvalue of $J_c + \bar{A}_{c1}$
ξ	non-dimensional co-ordinate of pipe

ξ_b	non-dimensional location of constraint
ρ, $\tilde{\rho}$	variables defined in Eqs. (32) and (29b)
$\bar{\rho}$	the value of ρ at equilibrium
σ_i	coefficient defined in Eq. (3)
τ	non-dimensional time
φ	phase angle of solution
$\varphi_i(\xi)$	ith eigenfunction of cantilevered beam
φ_f, φ_I, φ_R	coefficients defined in Eq. (45)
ω_0	$\sqrt{H_3/H_1}$
ω_1	imaginary part of υ_2
Ω, Ω_i,	eigenvalues of A_{μ_0}

References

[1] M.P. Païdoussis, G.X. Li, Pipes conveying fluid: a model dynamical problem, Journal of Fluids and Structures 7 (1993) 137–204.

[2] M.P. Païdoussis, F.C. Moon, Non-linear and chaotic fluidelastic vibrations of a flexible pipe conveying fluid, Journal of Fluids and Structures 2 (1988) 567–591.

[3] M.P. Païdoussis, G.X. Li, F.C. Moon, Chaotic oscillations of the autonomous system of a constrained pipe conveying fluid, Journal of Sound and Vibration 135 (1989) 1–19.

[4] M.P. Païdoussis, G.X. Li, R.H. Rand, Chaotic motions of a constrained pipe conveying fluid: comparison between simulation analysis and experiment, Journal of Applied Mechanics 58 (1991) 559–565.

[5] M.P. Païdoussis, J.P. Cusumano, G.S. Copeland, Low-dimensional chaos in a flexible tube conveying fluid, Journal of Applied Mechanics 59 (1992) 196–205.

[6] J.D. Jin, Stability and chaotic motions of a restrained pipe conveying fluid, Journal of Sound and Vibration 208 (1997) 427–439.

[7] J. Carr, Applications of Center Manifold Theory, Springer New York, 1981.

[8] J.D. Jin, Y. Matsuzaki, Bifurcation analysis of double pendulum with a follower force, Journal of Sound and Vibration 154 (1992) 191–204.

[9] J. Guckenheimer, P. Holmes, Non-linear Oscillations, Dynamical System and Bifurcation of Vector Fields, Springer, New York, 1983.

[10] P.R. Sethna, S.W. Shaw, On codimension-three bifurcations in the motion of articulated tubes conveying fluid, Physica D 24 (1987) 305–327.

[11] G.X. Li, M.P. Païdoussis, Stability, double degeneracy and chaos in cantilevered pipes conveying fluid, International Journal of Non-Linear Mechanics 29 (1994) 83–107.

[12] F.C. Moon, Chaotic Vibrations, Wiley, New York, 1987.

[13] S. Wiggins, Introduction to Applied Non-linear Dynamical Systems and Chaos, Springer, New York, 1990.